Effect of Degenerate Semiconductor Band Structure on Current-Voltage Characteristics of Silicon Tunnel Diodes

R. A. LOGAN AND A. G. CHYNOWETH
Bell Telephone Laboratories, Murray Hill, New Jersey
(Received 3 January 1963)

The three components of the band-to-band tunnel current of silicon Esaki junctions at low temperatures, the phonon-unassisted current i_0, the TA phonon-assisted current i_1, and the TO phonon-assisted component i_2, have been derived from the experimental current-voltage characteristics by an empirical, but extremely self-consistent, technique. The components are in constant ratio to each other for a given donor species but junctions formed using Sb gave relatively lower i_0 currents than did junctions formed with P- or As-doped material. The three current components have very similar bias dependence which, empirically, turns out to be accurately described by $V\exp(-\beta' V)$, where β' is a constant for a given junction. Part of the exponential factor represents the bias dependence of the tunneling probability, the remainder enters into the "effective density of states" function. The true peak voltage is given by $1/\beta'$. The experimental current-voltage curves are compared with each of Kane's theories; the first is for undistorted band edges while the second takes account of the band edge tails in very impure semiconductors. Good agreement is obtained using the latter theory, both as to the over-all shape of the curves and the actual values of the peak voltages.

I. INTRODUCTION

THE description of the shape of the current-voltage (I-V) characteristic of a tunnel diode in terms of a smooth "uncrossing" of the energy bands is well known. In the simplest analysis, the tunnelling probability is assumed constant over the relatively narrow forward bias range where band-to-band tunnelling occurs and then the I-V characteristic is determined by the "overlap" integral, over the appropriate energy range, of the product of the electron and hole densities on the two sides of the junction. Such an analysis was first given by Esaki[1] who made the natural assumption for a first approximation that the densities of states varied as (energy)$^{1/2}$ in the two energy bands. With this assumption, Esaki obtained fair agreement with experimental data. However, it is now generally appreciated that the assumptions of (i) constant tunnelling probability and (ii) parabolic energy bands are very poor ones in practice. Furthermore, (iii) the simple evaluation of the overlap integral does not take into account the need for transverse momentum to be conserved in the tunnelling transition, and (iv) it ignores the group velocity of the carriers in the field direction. When the corrections are included, the evaluation of the overlap integral becomes more complicated though this has been done by Kane for both direct and indirect transitions.[2] While retaining the first two assumptions given above, Kane finds that, depending on the magnitudes of the Fermi energies on the two sides of the junctions, the I-V characteristics could either be roughly trapezoidal in shape, with a relatively broad, flat peak, or more sharply peaked. In either case, the peak current should be reached at a bias, V_P, roughly comparable to $\zeta_{\min}$, the lower of the two Fermi energies.

More recently, Kane[3] has extended the theoretical treatment to include one possible cause of distortion from a (energy)$^{1/2}$ density-of-states distribution, namely, the effect of local statistical fluctuations in the impurity density. He uses a model in which the effect of a locally higher-than-average impurity concentration imparts a local lowering of the potential, and vice versa. As a result, the energy distribution of local band edges will be Gaussian and this represents, in effect, the phenomenon of a band edge tail when a summation is made over the whole area though the local density of states will remain proportional to (energy)$^{1/2}$.

It is of interest to compare the I-V characteristics predicted by Kane's old and new theories with experimental results. To do so requires the use of a material where the junction fabrication process is under adequate control and where the impurity concentrations on the two sides of the junction are known with reasonable accuracy. On account of previous work, silicon met these requirements. However, the interpretation of data from silicon junctions is complicated by the fact that the tunnelling transitions are indirect. Tunnelling with the emission (or absorption) of a phonon introduces an effective bias shift (equivalent to the phonon energy) into the current-voltage characteristics[4–6] and empirical techniques were devised for decomposing the characteristics measured at 4.2°K into the separate phonon-assisted and phonon-unassisted components in the bias range where band-to-band tunnelling is occurring.

As a result of this decomposition, new meaning was given to V_P, the actual peak voltage, and in particular, the important role played by the bias dependent tunnelling probability in determining the over-all shape of the I-V characteristic was clearly brought out. In Secs. II and III the experimental aspects of this work will be described and the I-V data presented. The shapes of the I-V characteristics will be analyzed in

[1] L. Esaki, Phys. Rev. **109**, 603 (1958).
[2] E. O. Kane, J. Appl. Phys. **32**, 83 (1961).
[3] E. O. Kane, preceding paper, Phys. Rev. **131**, 79 (1963).
[4] R. N. Hall, J. H. Racette, and H. Ehrenreich, Phys. Rev. Letters **4**, 456 (1960).
[5] L. Esaki and Y. Miyahara, Solid-State Electron. **1**, 13 (1960).
[6] A. G. Chynoweth, R. A. Logan, and D. E. Thomas, Phys. Rev. **125**, 877 (1962).

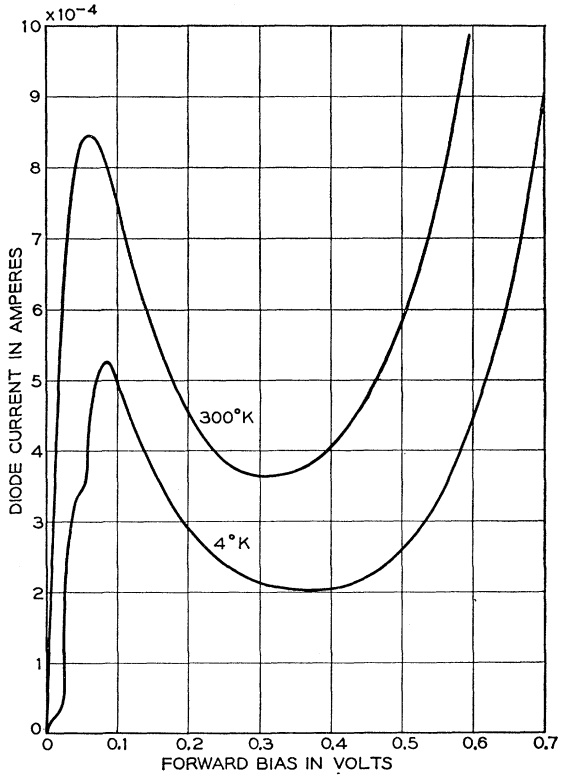

FIG. 1. The current-voltage characteristics of a typical silicon tunnel diode at 300 and 4°K.

Sec. IV and an empirical relation between I and V will be derived. In Sec. V, the experimental I-V characteristics are compared with the predictions of each of Kane's theories.

II. EXPERIMENTAL

The diodes were made by alloying Al wires containing 1% of boron into small cubes of n-type Si using a fast heating cycle in which a maximum temperature of about 725°C was reached. The resistivity of the regrowth region was found to be 0.005 Ω-cm by direct measurement. This corresponds to an acceptor concentration of 2.3×10^{19} cm^{-3} and is about an order of magnitude smaller than previous estimates based simply on equilibrium solid solubility data. The n-type silicon was doped with either P, As, or Sb and the donor concentration was determined from Hall-effect measurements on the same pieces in which the diodes were subsequently made. Contact to the n-type material was made by a gold wire alloyed to it. The alloying cycle and the ensuing junction areas (3.5×10^{-4} cm^2) were essentially identical for all the diodes. However, the current densities of diodes made on the same substrate material were found to vary in a range of $\pm20\%$ about an average value. It is believed that this was caused principally by inhomogeneity in the aluminum-boron wire. The diodes were not etched or further processed after the alloying step.

The I-V characteristics were recorded on an X-Y recorder using a conventional four-wire technique. In those cases where the peak voltage was measured, the diode was stabilized by a shunt resistor and the actual diode characteristic was then recorded using a circuit designed by D. E. Thomas which automatically subtracted the current through the shunt resistor. Data at 4.2°K were obtained with the diode immersed in liquid helium.

III. RESULTS

Figure 1 shows the I-V characteristics of a typical diode both at room temperature and at 4°K. It will be noted that in going from room temperature to 4°K: (i) the discontinuities due to the phonons become prominent; (ii) the bias V_P corresponding to the peak current increases considerably; (iii) the peak current, I_P, decreases considerably and (iv) the valley current, I_V, decreases by a proportional amount. Previous work[7,8] has shown that the changes in I_P and I_V can be accounted for by the temperature dependence of the energy gap and the phonon density.

The dependence of the forward current density at room temperature and at a fixed bias of 0.025 V upon

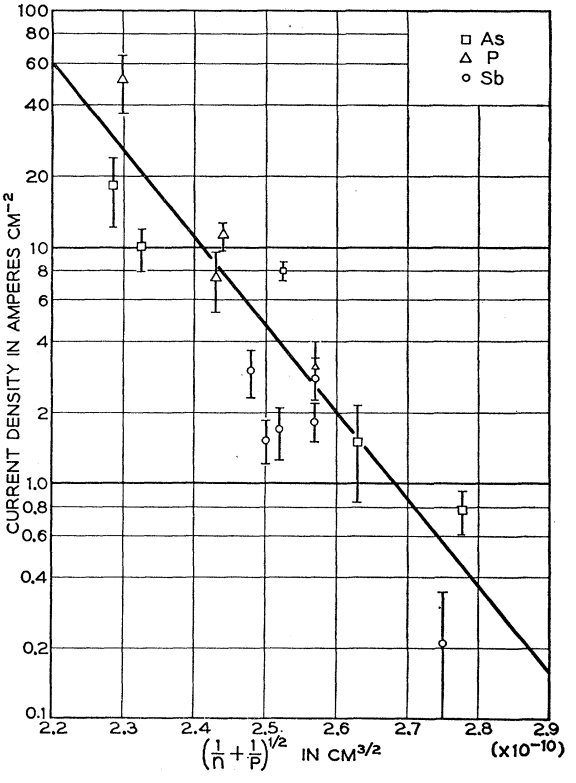

FIG. 2. Semilogarithmic plot of the band-to-band tunnel current vs the junction width parameter at room temperature.

[7] A. G. Chynoweth, W. L. Feldmann, and R. A. Logan, Phys. Rev. **121**, 684 (1961).

[8] A. G. Chynoweth, W. L. Feldmann, C. A. Lee, R. A. Logan, G. L. Pearson, and P. Aigrain, Phys. Rev. **118**, 425 (1960).

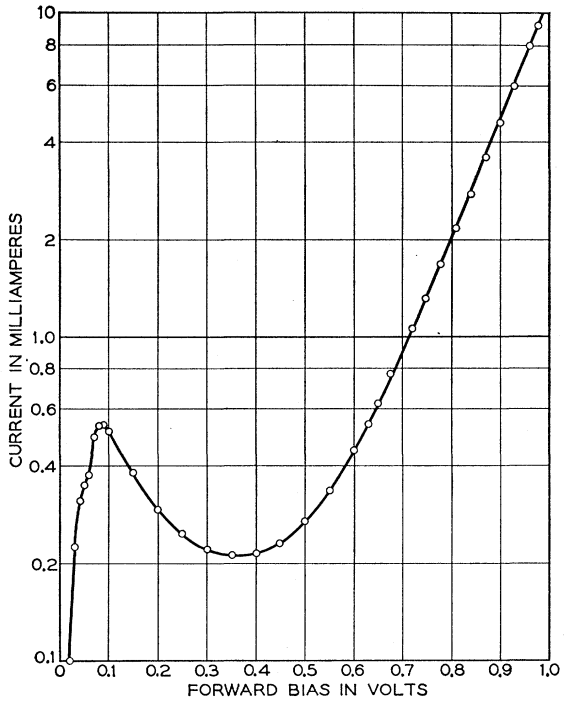

FIG. 3. Semilogarithmic plot of the current-voltage characteristic at 4°K shown in Fig. 1.

junction width (more precisely $[(n+p)/np]^{1/2}$, a parameter proportional to the junction width for unit potential drop across it, n and p being the net donor and acceptor concentrations on the two sides of the junctions, respectively) is shown in Fig. 2, the data being taken at room temperature. It is apparent that to within the precision of the data the current does not depend upon the specific n-type dopant used. As described above, each current density represents an average obtained from six diodes made from the same substrate material; the mean deviation observed is also indicated. As will be discussed more fully later, the slope of the straight line drawn through the experimental points leads to a value of the exponent in the familiar exponential tunnelling probability factor. (The peak current could have been plotted instead of I at 0.025 V. This would have resulted in a parallel set of data since the ratio of these two currents was always the same from unit to unit. However, in unstabilized circuits, the junction is unstable at the peak current and this tends to make its location slightly less accurate than, say, the current at 0.025 V.)

While the band-to-band tunnel current did not show any marked dependence on dopant, this was less true of I_V. On the average, the peak-to-valley ratio, $R=I_P/I_V$, varied with dopant as follows: Sb, 1.94 ± 0.23; As, 1.53 ± 0.30; P, 1.16 ± 0.10, where the mean deviations are indicated. Thus, for any given peak current or doping concentration), the valley current (or excess current) is highest for the phosphorus-doped samples and lowest for the antimony-doped samples. This effect was also observed in silicon junctions by Holonyak *et al.*[9] and in germanium junctions by Longo[10] where it was observed that greater values of R were obtained with As-doped than with P-doped samples. The reason for this variation with specific dopant has not been established though a current model of the excess current mechanism[7] leads to the conclusion that the density of gap states introduced by the dopants increases along the series Sb, As, P in both Si and Ge.

Figure 3 shows a semilogarithmic plot of the curve for 4°K shown in Fig. 1. As has been discussed in detail elsewhere,[7] such a plot exhibits an extensive linear portion in the bias range where the excess current is dominant and the slope of the straight line involves the exponent in the barrier transparency factor. This plot is typical for the class of diodes considered here where both the n and p regions of the junction are sufficiently heavily doped that the forward characteristics have well-defined peaks and valleys. Hence, in general, if this linear excess current region can be extrapolated to lower biases, it will be seen that at biases $\leq V_P$, the amount of excess current is negligible compared with the total current (conceivably, some tunnel current can still flow by way of gap states even when the bands are not uncrossed). Thus, at biases $\leq V_P$, the total tunnel current represents, with reasonable certainty, the band-to-band tunnel current. Furthermore, the value of V_P will not be influenced to any significant extent by the background excess current.

The dependence of V_P upon donor concentration, as determined from the I-V traces is shown in Fig. 4 for room temperature and 4°K. Again to within the experimental precision there is no correlation between

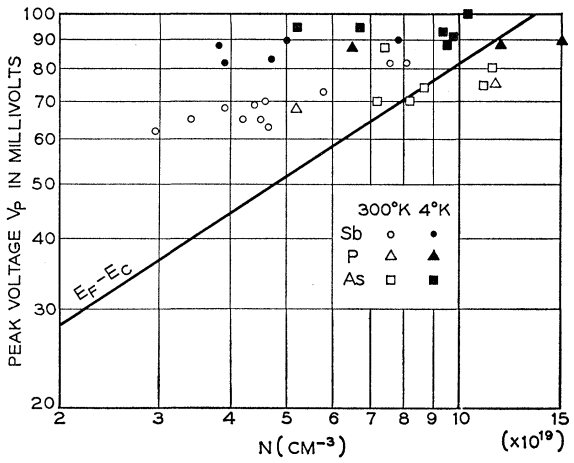

FIG. 4. The dependence of the peak voltage, V_P, of the I-V characteristic on the donor concentration at 300 and 4°K. The straight line represents the Fermi energy.

[9] N. Holonyak, Jr., D. C. Jillson, and S. F. Bevacqua, *Metallurgical Society Conferences* (Interscience Publishers, Inc., New York, 1961), Vol. 12, p. 81.

[10] T. A. Longo, Bull. Am. Phys. Soc. **5**, 160 (1960).

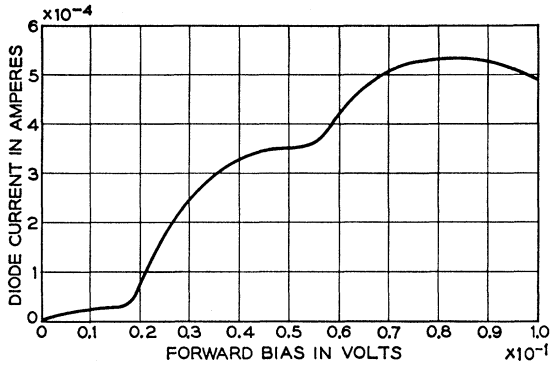

FIG. 5. Initial segment of the I-V characteristic at 4°K shown in Fig. 1.

V_P and the specific n-type dopant. Furthermore, V_P is relatively insensitive to donor concentration, especially at low temperatures. Also, at room temperature, the total variation of V_P over the range of impurity densities covered is from about 0.062 to 0.085 V, whereas the Fermi energies for the corresponding impurity concentrations range from 0.037 to 0.090 eV.

Figure 5 is an enlargement of the initial portion of the I-V characteristic at 4°K shown in Fig. 1. The current that flows in the bias range 0–0.018 V is loosely termed the phonon-unassisted current. At 0.018 V, the transverse acoustic (TA) phonon-assisted current begins while the transverse optic (TO) phonon-assisted current begins[6] at 0.058 V. To compare the relative magnitudes

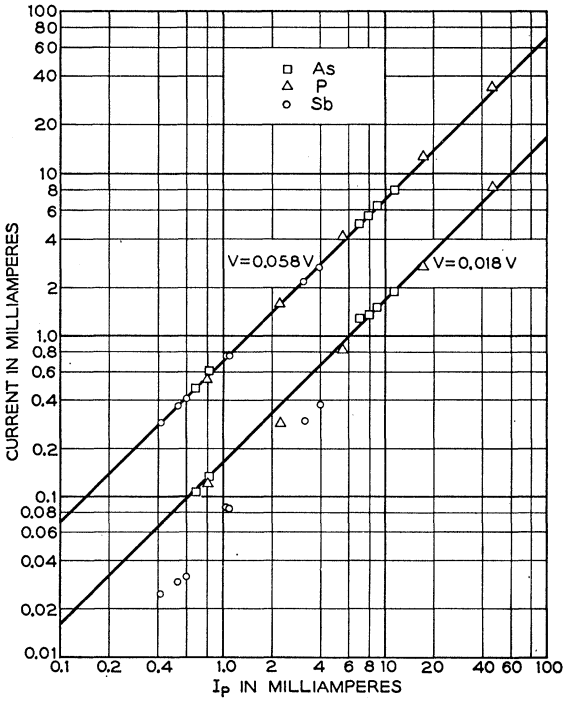

FIG. 6. Plots of the currents at various particular biases vs the peak current for junctions of different doping concentrations and dopant.

of the phonon-assisted and phonon-unassisted currents as a function of impurity concentration, the current magnitudes at 0.018 and 0.058 V were plotted against I_P with the results shown in Fig. 6; it is clear that, again to within the precision of the experiments, the I-V characteristics scale closely to each other throughout the doping concentration range covered. In particular, the unassisted current shows the same variation with junction width as do the assisted currents. However, it is evident that the magnitude of the unassisted current is less for the Sb-doped diodes than for the As- and P-doped diodes.

IV. ANALYSIS

Figure 5 clearly demonstrates that for forward biases $\leq V_P$, the forward tunnel current is the sum of three components. The first component, i_0, is the tunnel current that flows without phonon participation and this component accounts for all the observed current for biases less than approximately 18 mV, corresponding

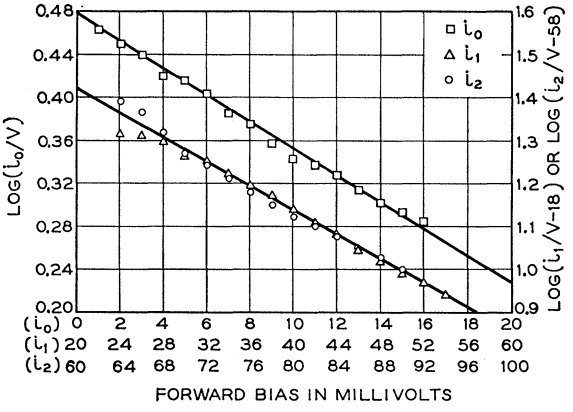

FIG. 7. Plots of the $\ln(I/V)$, etc., against V, which establish the validity of the empirical function, $I \sim V \exp(-\beta' V)$.

to the TA phonon. If it were not for the phonon-assisted current components, i_0 would be seen to peak at a bias somewhat greater than 18 mV and thereafter pass into a negative resistance region. At 18 mV, the TA phonon-assisted component, i_1, starts so that the total observed current is then $i_0+i_1=i_1'$, say. The i_1 component alone would also be expected to follow a hump-shaped curve somewhat similar to that of i_C. However, at 58 mV a third component, i_2, is added due to TO phonon-assisted tunnelling, the total current then being denoted by $i_2'=i_0+i_1+i_2$. The major aim in this work was to derive the separate components, i_0, i_1, and i_2, and to compare their shapes with those predicted by Kane.

To separate the current components it is necessary to know their functional form. Kane has shown that the bias dependence of the current can be expressed as

$$i(v) \sim F(V)D(V)P(V),$$

where $P(V)$ is the barrier transparency and $F(V)$ varies as (field)$^{3/2}$ and, hence, is essentially constant over the applied *bias* range of present concern. Unfortunately, the effective density-of-states function, $D(V)$, is too complex to allow any simple fitting of experimental and theoretical curves and so recourse was made to an empirical method for obtaining the separate components, i_0, i_1, i_2.

By trial and error, it was found that over the bias range, 0–18 mV, i_0 could be very well represented by a function of the form $V\exp(-\beta' V)$. When plots of $\ln(i_0/V)$ against V were made, they were found to be good straight lines over the whole bias range up to 0.018 V for all the junctions studied. [See Fig. 7. It is of interest to note that a linear dependence of $\ln(I/V)$ on V for the tunnelling current has also been found for Ge junctions for the forward-bias direction from zero through the negative resistance range[11] as well as in the reverse direction.[12] Both of these studies were confined to room temperature, however, and no attempt was made to separate the various phonon-assisted components. On the other hand, it is well known that most of the tunnel current in germanium junctions is carried by direct transitions.] It was then supposed that such plots could be extrapolated to somewhat higher biases at least, in which case, the extrapolated value for i_0 could be obtained; by subtracting i_0 from i_1', the component i_1 was determined. This component was likewise analyzed by plotting $\ln[i_1/V-0.018)]$ against V. Again a good straight line was always obtained and its slope, again supposedly β', was generally in excellent agreement with the value found from analyzing i_0. The whole procedure could be repeated again so as to derive component i_2, and it too was found to be a good straight line when $\ln[i_2/V-0.058)]$ was plotted against V.

A typical example of the three semilogarithmic plots for i_0, i_1, and i_2 is shown in Fig. 7. It is apparent that three good straight lines result and that their slopes are all in good agreement with each other. *This agreement clearly justifies the rather extensive extrapolations and the whole reiterative technique.* In particular, it is clear that, empirically, the voltage dependence of the current is very accurately described by $i\sim V\exp(-\beta' V)$. Moreover, it was found that this expression applied with similar precision over the whole range of junction widths used, with the true peak voltage, $V_p(=1/\beta')$, varying from 32 to 52 mV.

V. DISCUSSION

a. Band-to-Band Tunnel Current

Over the bias range 0 to 80 mV, the total band-to-band tunnel current is determined by the three components i_0, i_1, and i_2. As Fig. 6 demonstrates, for a given donor species, i_0, i_1, and i_2 are in roughly constant ratio to each other over the whole range of impurity concentrations covered. Figure 8 displays the three separate components as derived from the plots of Fig. 7, and it will be noted that i_1 is roughly comparable in magnitude to i_2. This is not surprising since, in the total expression for the tunnel current, there is no term that is *strongly* dependent on the phonon energy involved. Furthermore, we conclude that $|i_1|\simeq|i_2|$ irrespective of the donor species. On the other hand, while the current component i_0 remains in constant proportion to i_1 and i_2 for a given donor species, it is relatively smaller for the junctions doped with antimony. This parallels the relatively lower excess current noted in Sb-doped units and suggests that i_0 is possibly a tunnel current by way of gap states resulting, for example, from band edge tails.

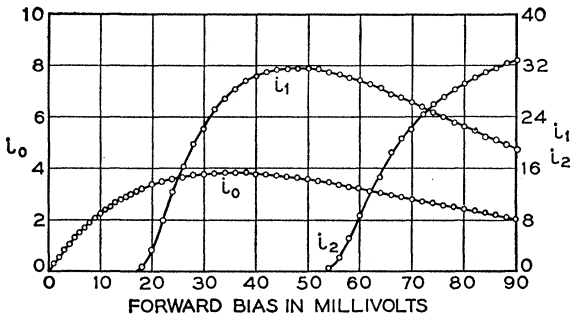

FIG. 8. Plots of the isolated current-voltage components that make up the total I-V characteristic.

It is apparent from Fig. 8 that the three current components all have very similar voltage dependence. This is brought out more clearly in Fig. 9 where the curves have been superimposed and scaled to each other. This similarity in shape confirms that the effect of the phonons is simply to generate a set of components with displaced origins and that the D function does not vary in form from one component to another.

The temperature dependence of the observed peak voltage, V_P, is now more clearly understood. At low temperatures V_P is determined principally by tunnelling

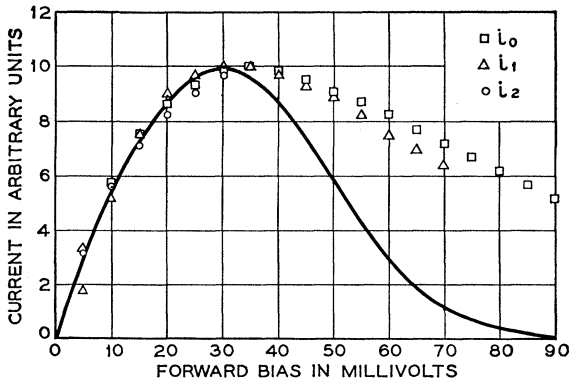

FIG. 9. The points represent the isolated current-voltage components scaled, and with their zeros adjusted so that the components superimpose. The solid line represents the I-V characteristic predicted by Kane's perfect crystal theory.

[11] A. Ferendeci and W. H. Ko, Proc. IRE **50**, 1852 (1962).
[12] M. I. Nathan, J. Appl. Phys. **33**, 1460 (1962).

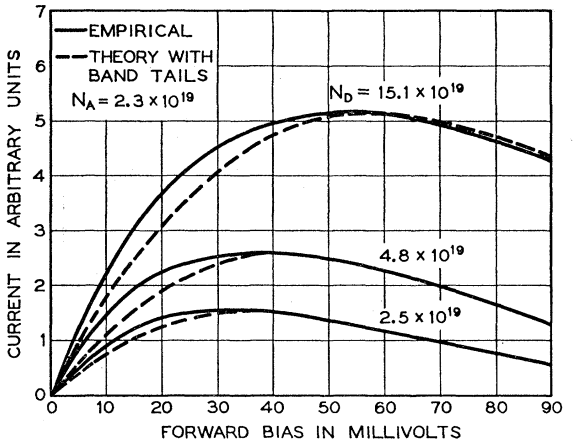

FIG. 10. Comparisons between the empirically derived current-voltage characteristics and theoretical curves computed by Kane using his band-edge tail theory. The pairs of curves are scaled to similar peak currents but there is no significance in the relative magnitudes of the curves.

transitions with phonon *emission*. The effective displacement of the origins of the i_1 and i_2 components by biases equivalent to the phonon energies then gives an apparently high value for V_P. At high temperatures, tunnelling can occur with phonon absorption; this makes V_P lower since the field does not then have to provide the phonon energy. A quantitative description of the temperature dependence of V_P, however, would have to take into account the Fermi occupancy function as well.

b. Quantitative Considerations

Above we have related $F(V)D(V)P(V)$ to $V\exp(-\beta' V)$, where $F(V)$ can be taken to be constant. To focus attention on $D(V)$ it is necessary to extract $P(V)$. For indirect tunnelling,

$$P(V)\simeq\exp\left(-\frac{\alpha\epsilon_G^{3/2}}{E}\right),$$

where

$$\alpha=4(2m_{rx}^*)^{1/2}/3e\hbar,$$

where ϵ_G is the forbidden energy gap, m_{rx} is the reduced effective mass in the tunnelling direction, e is the electronic charge, and h is Planck's constant. The field, E, can be taken as approximately two-thirds of the maximum field in a roughly symmetrical step junction[3] (one where the point of stationary phase coincides with the point of maximum field)

$$E=4(V_i-V)^{1/2}/3W_1,$$

where $V_i(\simeq\epsilon_G/e)$ is the built-in potential, V (positive) is the forward bias, and W_1 is the width constant of the junction given by

$$W_1=[K(n+p)/2\pi enp]^{1/2},$$

where K is the dielectric constant and p,n are the acceptor and donor concentrations, respectively. For small V we have

$$P(V)\simeq P(0)\exp(-\beta V),$$

where

$$\beta=3\alpha W_1 e^{3/2}/8.$$

From the slope of the line in Fig. 2 a value can be derived for the critical field, $\alpha\epsilon_G^{3/2}$. The value so obtained is $(3.1\pm0.6)\times10^7$ V-cm^{-1}, which is in fair agreement with that calculated using the reduced density-of-states mass, 2.2×10^7 V-cm^{-1}.

Using the value for $\alpha\epsilon_G^{3/2}$ found from Fig. 2, β was calculated to vary from 7 to 9 V^{-1} over the doping range used. Experimentally, the slopes of curves, such as those in Fig. 7, gave values of β' ranging from about 20 to 30 V^{-1}. In all cases, these values were considerably greater than the calculated values, β, and this disagreement is outside the precision of the experiments. Similar discrepancies were observed by Nathan[12] in reverse-bias tunnel current studies with germanium diodes. In view of the fair agreement between theory and experiment for the value of α, it is reasonable to place more reliance on the calculated values of β and to seek elsewhere for causes of the high values of β'. We note that, empirically, the various data could be made mutually consistent by adding another exponential factor of the form, $\exp(-\lambda V)$, to the expression for the tunnel current where λ is a constant with dimensions volt^{-1}. In this way the value of α as deduced from Fig. 2 would be left unchanged but the slopes of the lines in Fig. 7 would now be given by $-\beta'=-(\beta+\lambda)$. Thus, empirically, we now have $D(V)\sim V\exp(-\lambda V)$, where λ ranges between 15 and 21 V^{-1} over the doping range covered.

It might be noted that a similar decomposition of an exponential factor into two exponential factors was proposed in connection with the problem of excess currents in silicon junctions.[7] The first exponential which is included in the D factor is, essentially, a function of energy (or bias) only, while the other exponential factor describing the tunnelling probability is a function of junction width and temperature as well as bias. Thus, the "β" determined from the temperature or junction width dependence of the current *at fixed bias* is found to be greater than that obtained from the *bias dependence* of the current.[7]

c. Comparisons with Theory

We wish to make direct comparisons between the empirically derived current components and the I-V characteristics predicted by Kane's old[2] and new[3] theories, referred to as K1 and K2, respectively.

For the junction whose current components are shown in Fig. 10, the "perpendicular energy," $\bar{E}_\perp$ was estimated to be 0.047 eV and the Fermi energies on the n and p sides were 0.041 and 0.051 eV, respectively. Allowing for $P(V)$ in the way described in K2, the

product $D(V)P(V)$ was computed using Eqs. (35), (36), and (37) of K1. The theoretical current is practically proportional to this product and the theoretical curve is shown in Fig. 9 normalized to the same peak current as the empirical curves. Clearly, agreement is good up to about the peak voltages, but at higher biases the theoretical curve drops off very much faster than the experimental one. The reasonable conclusion is that the substained experimental currents arise from the presence of band edge tails so that a clean uncrossing of the energy bands does not occur.

Kane has used his band-edge tail theory (K2) to compute the theoretical current-voltage curves for three representative junctions. These junctions cover the range of donor concentrations used in these experiments, namely, 2.5×10^{19}, 4.8×10^{19}, and 1.5×10^{20} cm^{-3}. For all three junctions the acceptor concentration was 2.3×10^{19} cm^{-3}. The true peak voltages found experimentally for these three junctions were 33, 36, and 52 mV. Kane's theory leads to values of 36, 42, and 56 mV, respectively, in good agreement with the experimental values. The empirical curves, $V\exp(-\beta' V)$ with $\beta'=V_p^{-1}$, are compared with the theoretical ones in Fig. 10. For each junction the pairs of curves have been normalized to have the same peak current but the relative magnitudes for the three junctions have no significance. It is clear that in addition to the agreement of peak voltages, the theoretical curves are a good fit to the experimental ones at biases greater than the peak voltage, in contrast to the earlier theory, K1, for undistorted bands. No particular significance can be attached to the slight discrepancies at low biases.

The authors wish to express their appreciation to E. O. Kane for many valuable discussions.

PHYSICAL REVIEW VOLUME 131, NUMBER 1 1 JULY 1963

Mechanism of Second Harmonic Generation of Optical Maser Beams in Quartz

ROBERT C. MILLER
Bell Telephone Laboratories, Murray Hill, New Jersey
(Received 18 February 1963)

This paper is concerned with the experimental determination and the interpretation of the relative magnitudes of the two independent coefficients, d_{11} and d_{14}, that appear in the tensor which describes the symmetry of second harmonic generation (SHG) of optical maser beams in quartz. Experimental data on these coefficients aid in determining the physical process involved in optical SHG. Data have been obtained for both ruby (6934 Å) and $CaWO_4$:Nd^{+3}(10 582 Å) unfocused laser beams. These experiments, which failed to give any evidence of SHG due to d_{14}, show that $d_{14}/d_{11}<1/30$ for the ruby laser, and $<1/40$ for the Nd laser. The result $d_{14}\ll d_{11}$ shows that the mechanism involved in SHG in quartz is nearly lossless and dispersionless at the frequencies of the laser beams and their second harmonics. This further shows that in quartz the linear electro-optic effect and optical SHG cannot be due to the same mechanism. It is concluded that optical SHG in this material is due to a high-frequency electronic mechanism.

INTRODUCTION

THERE exists in the literature a fair amount of experimental data[1–4] and theoretical discussion[5–8] on frequency doubling of optical maser beams in quartz. Of particular theoretical interest is the paper by Kleinman[5] which indicates that insight into the mechanism involved in second harmonic generation (SHG) can be obtained from experimental data on the symmetry of the phenomenon. The required data have now been obtained for SHG of the ruby and $CaWO_4$:Nd^{+3} laser beams in quartz. The method by which these data have been determined, and their interpretation in terms of the mechanism responsible for SHG in quartz, are discussed in this paper.

From the point group of quartz, class D_3, it can be shown[1] that the second order polarization, $\mathbf{P}_{2\omega}$, has the form,

$$\mathbf{P}_{2\omega}=\begin{bmatrix} d_{11} & -d_{11} & 0 & d_{14} & 0 & 0 \\ 0 & 0 & 0 & 0 & -d_{14} & -2d_{11} \\ 0 & 0 & 0 & 0 & 0 & 0 \end{bmatrix}\begin{bmatrix} E_x^2 \\ E_y^2 \\ E_z^2 \\ E_yE_z \\ E_xE_z \\ E_xE_y \end{bmatrix}. \quad (1)$$

In Eq. (1), $\mathbf{P}_{2\omega}$ is the part of the dielectric polarization that varies with time at twice the laser frequency ω, E_i are the optical electric field components in the medium at frequency ω, and d_{ij} are the nonlinear coefficients. There has been some speculation concerning the magni-

[1] P. A. Franken, A. E. Hill, C. W. Peters, and G. Weinreich, Phys. Rev. Letters **7**, 118 (1961).
[2] P. D. Maker, R. W. Terhune, M. Nisenoff, and C. M. Savage, Phys. Rev. Letters **8**, 21 (1962).
[3] B. Lax, J. G. Mavroides, and D. F. Edwards, Phys. Rev. Letters **8**, 166 (1962).
[4] A. Savage and R. C. Miller, Appl. Opt. **1**, 661 (1962).
[5] D. A. Kleinman, Phys. Rev. **126**, 1977 (1962).
[6] J. A. Armstrong, N. Bloembergen, J. Ducuing, and P. S. Pershan, Phys. Rev. **127**, 1918 (1962).
[7] P. A. Franken and J. F. Ward, Rev. Mod. Phys. **35**, 23 (1963).
[8] D. A. Kleinman, Phys. Rev. **128**, 1761 (1962).